Geochemistry Geophysics Geosystems G3
AN ELECTRONIC JOURNAL OF THE EARTH SCIENCES
Published by AGU and the Geochemical Society

Characterization
Volume 5, Number 9
1 September 2004
Q09001, doi:10.1029/2004GC000690
ISSN: 1525-2027

Top of the crystalline basement in the Levant

Michael Rybakov
Geophysical Institute of Israel, P.O. Box 182, Lod 71100, Israel

Amit Segev
Geological Survey of Israel, 30 Malkhei Israel Street, Jerusalem 95501, Israel (amit.segev@mail.gsi.gov.il)

[1] A structural map of depth to the top of the crystalline basement has been constructed for the Middle East continental and marine terrains by reviewing available relevant information on the Levant (deep boreholes, seismic profiles, and magnetic and gravity data (and adopting the regional compilation of Cornell University for the adjacent areas. This new compilation enabled significant upgrading of the Cornell University database for the Levant with emphasis on Israel. The present top of the crystalline basement map gives a good large- and medium-scale overview on the basement relief of a complex area that includes (1) the African and Arabian continental platforms; (2) the Mesozoic Levant passive continental margins; (3) the Mesozoic Syrian arc and the Palmyrides fold belt and rifts; (4) the Cenozoic Cyprus collision zone; (5) the Alpine orogenic belt of Turkey; (6) the Red Sea oceanic spreading center and the Suez rift; and (7) the Dead Sea Transform.

Components: 4347 words, 2 figures, 1 table.

Keywords: Middle East; Levant; top basement.

Index Terms: 0905 Exploration Geophysics: Continental structures (8109, 8110); 8105 Tectonophysics: Continental margins and sedimentary basins (1212)

Received 13 January 2004; **Revised** 20 June 2004; **Accepted** 18 July 2004; **Published** 1 September 2004.

Rybakov, M., and A. Segev (2004), Top of the crystalline basement in the Levant, *Geochem. Geophys. Geosyst.*, *5*, Q09001, doi:10.1029/2004GC000690.

1. Introduction

[2] The basement of the continental parts surrounding the eastern Mediterranean area (Figure 1) is part of the northern Arabian Nubian Shield (ANS), which formed during the Neoproterozoic orogenic cycle (Pan-African) [*Bentor*, 1985; *Stern*, 1994; *Stein and Goldstein*, 1996] and ended in the Early Cambrian ca. 532 Ma [*Segev*, 1987; *Beyth and Heimann*, 1999; *Mushkin et al.*, 1999]. At that time the study area (Levant) was located in the northern part of Gondwana, but later, during the Variscan (Hercynian) orogeny, collided with Laurussia, and was broken up several times to continental fragments since then [*Sengör et al.*, 1984; *Segev*, 2000, 2002; *Stampfli*, 2000]. The relief of the top crystalline basement in the Middle East was thus formed mainly during the Phanerozoic Era. The Cenozoic structural elements are relatively well preserved.

[3] Our new top of the crystalline basement map is based mainly on a comprehensive review of the relevant data within Israel, Jordan, Sinai and NE Egypt (within green frame in Figure 1), which is part of a recent study of the Levant lithospheric structure by *Segev et al.* [2003]. *Makris and Wang* [1995] presented a 3-D map of depth to the basement in the eastern Mediterranean Sea based mainly on experiments of deep seismic sounding. This map shows a few large-scale features, such as basement highs under Cyprus and the Eratosthenes Seamount, and lows in the Levantine basin and the vicinity of the Anaximander Seamount. The team at the Institute for the Study of the Continents at

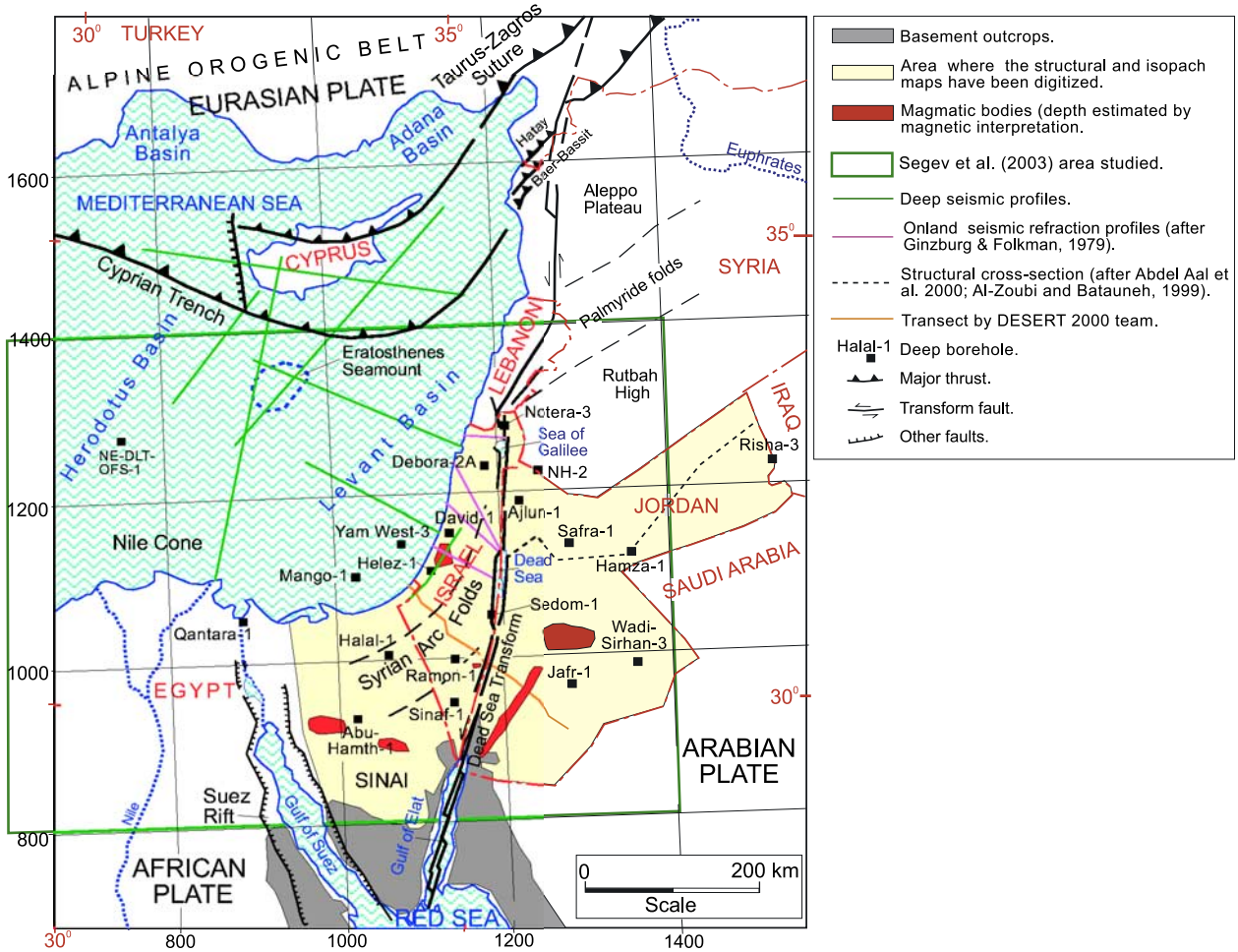

Figure 1. Location and source map displaying the geography, main tectonic features (plates and fault systems), and the location of deep seismic profiles, boreholes, and magmatic bodies used for calculating the depth to the crystalline basement.

Cornell University (Barazangi, Gomez, Brew, Seber, Sandvol, Steer, Vallve, Orgren, Fielding, Isaacs and others) recently prepared a more detailed regional compilation map of the top crystalline basement, which includes also the continental parts. They collected a considerable amount of geophysical and geological data on the Middle East and organized it into a comprehensive open GIS database. Their grid spacing of depth to basement values is about a 1 arc minute, which corresponds roughly to 2 km at the Levant latitude, although the actual data spacing is much larger. The Cornell University basement grid was used in the present compilation as an initial data set to be detailed. *Rybakov et al.* [1999a] compiled their top crystalline basement map of central Israel on the basis of the Helez Deep-1A borehole, which penetrated the basement, seismic reflection profiles [*Trachtman et al.*, 1990], structural data of the Mesozoic strata, 3-D gravity back stripping, and magnetic interpretation. Information from the Gevim-1 borehole drilled recently has subsequently confirmed this structural map. Our new map reflects the overall geological processes that significantly affected and produced the basement elevation of the study area.

2. Sources and Methods

[4] Several studies published recently concerning basement data on Israel and adjacent areas (Figure 1) presented detailed and accurate maps. These and the various types of source data used are described below.

2.1. Deep Boreholes

[5] The most reliable data are from deep boreholes [*El Beialy*, 1988; *Abu Ollo and El Kholy*, 1992;

Table 1. Data Points of Depth to the Crystalline Basement of Boreholes, Magnetic Causative Bodies, and Seismic Profiles

Data Points	Coordinate		Depth to Basement, km	Disparity,[a] km
	East	North		
		Boreholes		
Abu-Hamth-1	1019	932	2.2	0.1
Ajlun-1	1223	1189	2.6	0.1
David-1	1138	1153	>6.0	
Debora-2a	1182	1233	>5.5	
Gevim-1	1112	1100	4.6	0.2
Halal-1	1059	1007	>5.5	
Hamza-2	1358	1122	>4.0	
Helez-d-1	1114	1109	6.1	0.4
Jafr-1	1280	965	3.2	0.1
Mango-1	1022	1103	>4.7	
NE-DLT-OFS	746	1276	>6.5	
NH-2	1246	1225	>5.0	
Notera-3	1208	1281	>3.0	
Qantara-1	885	1052	>4.2	
Ramon-1	1138	1001	>3.5	
Risha-3	1530	1229	>4.5	
Safra-1	1280	1137	1.8	0.1
Sedom-Deep-1	1186	1053	>6.5	
Sinaf-1	1136	949	>1.0	
Wadi-Sirhan-3	1360	989	>4.5	
Yam-West-2	1078	1142	>5.3	
		Magnetic Causative Bodies		
1	1272	1024	2.5	0.4
2	1240	987	1.9	0.3
3	1166	886	−0.8	0.1
4	1058	904	1.3	0.3
5	984	927	1.9	0.2
6	1163	994	2.5	0.5
7	1127	1126	6.1	0.8
		Seismic Profiles: Edges		
Profile I West	1151	1268	6.6	0.4
Profile I East	1205	1265	7.3	0.5
Profile II Northwest	1140	1246	6.5	0.1
Profile II Southeast	1198	1129	7.7	0.7
Profile III Northwest	1128	1195	6.9	0.2
Profile III Southeast	1197	1127	7.1	0.9
Profile IV Northwest	1108	1141	6.9	0.6
Profile IV Southeast	1188	1095	5.9	1.1

[a] Disparity between the actual depth of the boreholes and depth calculated from the basement grid.

Alfy et al., 1992; *Abu Saad and Andrews*, 1993; *Abdel Aal et al.*, 1994; *Rybakov et al.*, 1999b; Y. Folkman, personal communication, 2003]. A few deep boreholes (Helez Deep-1A, Besor-1 and Gevim-1 in Israel, the Abu Hamth-1 in the Sinai peninsula and the Ajlun-1, Safra-1 and Jaffr-1 in Jordan) penetrated the whole sedimentary succession and thus provided direct evidence of its total thickness. The other deep boreholes were used as constraints on the minimal basement depth estimations and for stratigraphic extrapolations. The data from the boreholes that penetrated the basement (Table 1) were used for constructing the grid and than to examine the disparity between this basement grid and the actual depth of the boreholes, which ranges from 0.1 km to 0.4 km. The density logs for the oil and water boreholes were used for interpreting sedimentary basins and for calculating a general depth-density function [e.g., *Rybakov et al.*, 1999b].

2.2. Seismic Profiles

[6] Four seismic refraction profiles performed in northern and central Israel (Figure 1) [*Ginzburg*

and Folkman, 1979] provided additional information on the depth to the basement. These data were reanalyzed using the results of a commercial seismic reflection survey carried out recently in northern Israel (T. Lutzkin, personal communication, 2003). Error estimations are given for the edges of each profile (Table 1). The calculated errors for the eastern edge of the profiles (close to the Dead Sea Transform) are generally higher than those for the western edge. For Israel, Jordan, and the Egypt-Sinai Peninsula (yellow polygons on the source map, Figure 1), we digitized the available structural and isopach maps [*Eyal et al.*, 1987; *Ryan*, 1978; *Andrews*, 1991, 1992a, 1992b; L. Kroiteru, personal communication, 2002]. These data enable obtaining the general pattern of the top of the crystalline basement by subtracting the total thickness of the Phanerozoic sedimentary succession from the topography. Recently, *Ben-Avraham et al.* [2002] reported on a seismic refraction/wide-angle reflection experiment along two lines crossing the continental shelf of Israel (Figure 1). The multidisciplinary transect DESERT 2000 that recently crossed the continental margin and the Dead Sea Transform (DST) provided valuable crustal information [*Weber and DESERT Group*, 2004]. The results of these studies (location and interpretations of the crustal structure) were digitized and added to our data set. The sedimentary thickness for the eastern Mediterranean [*Malovitsky et al.*, 1975] is also included in the present compilation. For the westernmost part of the region, the results of deep seismic soundings on the Herodotus abyssal plane (profile between Egypt and Rhodes from *Makris and Wang* [1995]) were taken into account even though they are located beyond the area studied. Structural cross sections, based on seismic profiles (western profile: *Abdel Aal et al.* [2000] and eastern profile: *Al-Zoubi and Batauneh* [1999]), were also taken into account. The latter profile was correlated with boreholes and thus provides information about the sedimentary sequence in northern Jordan.

2.3. Gravity Data

[7] Depths to the crystalline basement beneath the continental basins (Ghab, Bekka-Lebanon, Hula, Kinneret, Damia, Dead Sea, Timna, and Elat-Aqaba) along the Dead Sea Transform (DST) have been adjusted, using the results of the 3-D interpretation of the gravity data. The gravity anomalies (with magnitudes up to 140 mGal with respect to the surrounding mountains) are caused by young low-density sedimentary rocks overlying older, denser rocks [*ten Brink et al.*, 1999]. These gravity lows were inverted to estimate the thickness of young sediments, using the method developed by *Jachens and Moring* [1990]. The sedimentary basin parameters obtained from the automatic inversion were used as initial conditions for the 3-D forward modeling. The density logs of the deep oil and water boreholes provided important information for the gravity interpretation. *Rybakov et al.* [2003] described in detail the methodology used in the 3-D gravity interpretation. The reliability of the sedimentary thickness was verified using the forward modeling with an accuracy of 0.5–1.5 km. For the central part of Israel we used the top of the basement map prepared by *Rybakov et al.* [1999a], who used geological back stripping of the gravity data. The map produced has been calibrated and confirmed by the Helez Deep1A and the Gevim-1 boreholes, which penetrated the basement at a depth of 6.1 km and 4.5-km, respectively, as well as seismic reflection profiles [*Trachtman et al.*, 1990].

2.4. Magnetic Data

[8] Comparison of the geological and aeromagnetic data on the exposed crystalline basement (in southern Sinai, Eastern Desert of Egypt and Saudi Arabia) shows that Precambrian basic magmatics cause distinctive magnetic anomalies [*Folkman and Assael*, 1980]. Similar basic magmatics, covered by Phanerozoic sediments, should be identified by their low frequency magnetic anomalies. The interpretation of the aeromagnetic data therefore was used to provide additional information about the basement depth and its composition. We interpreted seven low frequency magnetic anomalies, which can be reliably identified as being caused by Precambrian magmatic bodies (red polygons in Figure 1). The 2-D Werner deconvolution technique [*Phillips*, 1997] was chosen for the first calculation of the depth to the magnetic causative bodies [*Rybakov et al.*, 2000]. This inverse solution obtains depth from the curvature of the magnetic field in comparison with the curvature produced by a reference model of an idealized geometric body. The clusters of the calculated depth values are indicative for a valid solution that appeared to be useful for the 3-D modeling at the second stage. This 3-D model, which is approximated by polygonal prisms, was compiled by an iterative 3-D MAGPOLY program [*Phillips*, 1997]. The iterative process was stopped when the main features of the calculated anomaly, the range and gradients, matched the observed one. At the last stage the subsurface models and the confidence intervals of

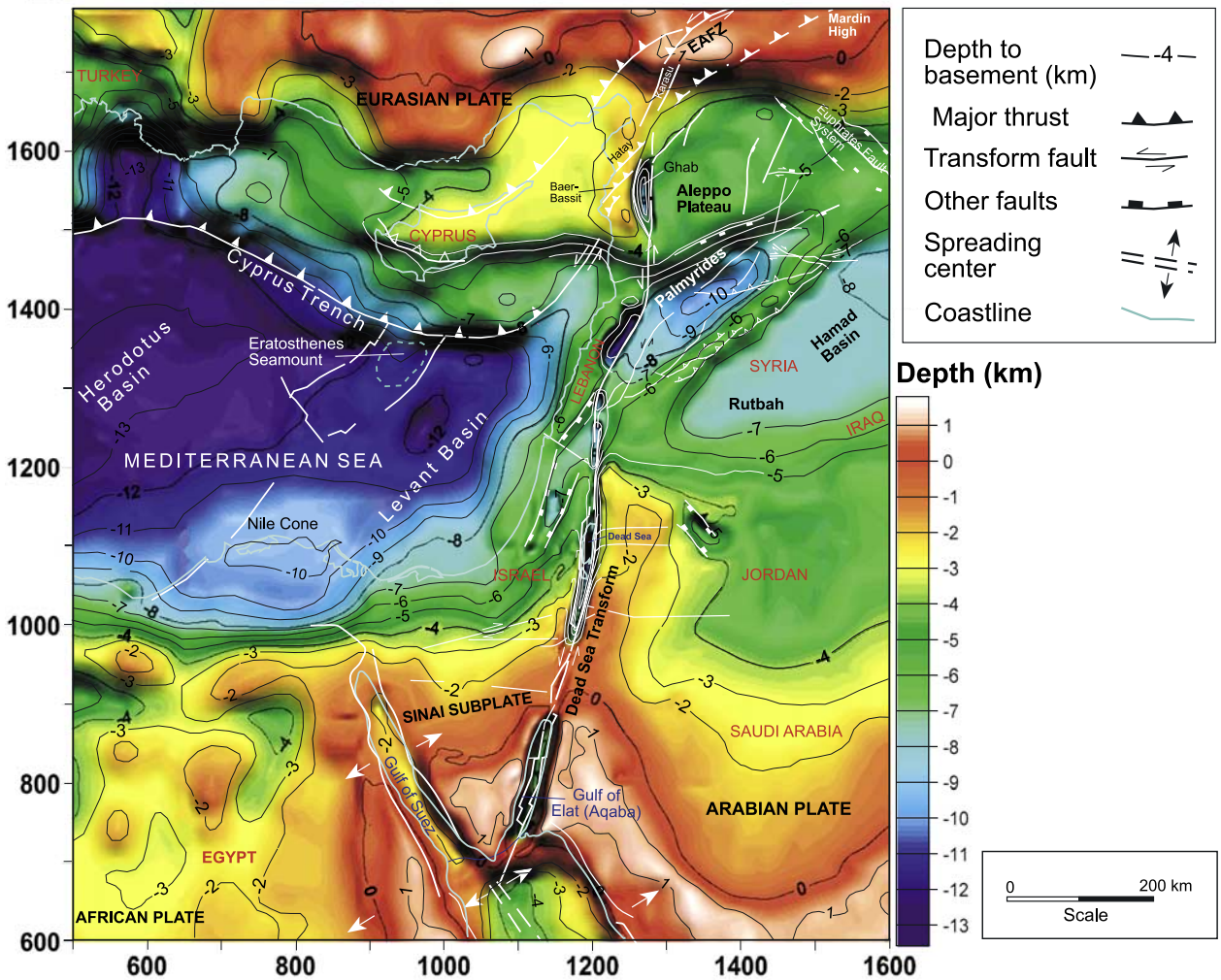

Figure 2. Top of the basement map (main faults after *Garfunkel and Bartov* [1977], *Garfunkel* [1981], *Ben-Avraham* [1985], *Brew et al.* [1997], and *Abdel Aal et al.* [2000]) emphasizing the general architecture of the Middle East tectonic plates (Africa, Sinai, Arabia, and Eurasia) and their boundaries (Dead Sea Transform, Gulf of Suez, Cyprus Trench, and the East Anatolian Fracture Zone).

the causative body parameters were processed using the 2.5-D and 3-D packages. Interactive modifications of model parameters enable designing the model as realistically as possible and estimating the confidence intervals of the model parameters. The present interpretation should be considered as a possible solution obtained from potential field data which is inherently not unique. Accuracy and reliability of the model parameters are strongly dependent on the correctness and reliability of the initial model and constraints. The appraisal of the calculated depths should be regarded as rough estimates. On the basis of realistic limitations for the parameters of the causative body and minimizing the misfit between the observed and calculated anomalies, we suggest the accuracy of the depth values to be about 0.5–1 km (Table 1). The coordinates shown in the table are related to the centers of the inferred isometric magnetic causative bodies. In the case of the large elongated bodies, the coordinates correspond to the locations of the minimal and maximal data points.

3. Top of the Basement Map

[9] The compiled map of depth to the crystalline basement is shown in Figure 2 as a contour map with hypsometric tints related to depth. All the direct and indirect measurements of depth to the crystalline basement were used as data points in the total data set. For interpolation between the

irregularly spaced data the inverse distance to a power method was applied. These were gridded with a node spacing of 2.5 km to show the relatively small lateral basement undulations. The file containing digitized fault traces was used in the gridding process. The two-dimensional fault file defines a line acting as a barrier to information flow when gridding. Data on one side of a fault is not directly used when calculating grid node values on the other side of the fault. This gridding was applied only for the largest faults of the Dead Sea Transform, which has a vertical displacement of ~5 km [*Hofstetter et al.*, 2000]. For large parts of the investigated area the estimated basement depth obtained is of ±1 km accuracy. It should be noted that a large discrepancy between the Cornell database and the present compilation is evident in the basement depth values along the Syria-Jordan border. The data from Syria appear to be about 2 km deeper than the data from Jordan. Taking into account the lack of structural data under the large Ash-Shaam volcanic field that covers this area, and on the basis of the Ajlun-1 borehole that penetrated the crystalline basement [*Abu Saad and Andrews*, 1993], the basement depth values in southernmost Syria were gradually aligned with the Jordanian data set. In regions where the crystalline rocks crop out at the surface, the relief elevations derived from the GTOPO30 data set were used in generating the basement topography. In the central part of Israel, the current model of the crystalline basement elevation is based on the grid recently published by *Rybakov et al.* [1999a].

4. Discussion

[10] The top of the crystalline basement map obtained (Figure 2) should be examined together with its source map (Figure 1) to see where the basement variability is supported by data. Generally, the top of the crystalline basement varies between approximately +2 km in the exposed Arabo-Nubian Shield and at the Alpine orogenic belt in the Tauride continental block and −13 km in the Herodotus basin, Mediterranean Sea. This wide range is mainly due to the structure of the Levant continental margins. A thick (±10 km) sedimentary succession, bottomed by Jurassic units, covers most of the southeastern Mediterranean oceanic crust (up to the Cyprus Trench). Steep continental margins characterize the Egyptian (south of the Nile cone) and the Lebanese margins (Figure 2). Discussion of the complicated structure north of the Cyprus Trench is beyond the scope of the present work.

[11] Before the updoming of the Red Sea structure since the Tertiary the southern continental parts of the Arabo-Nubian Massif were covered by relatively shallow (up to ±4 km) Phanerozoic sedimentary rocks. The Pan-African basin and swell structure [*Segev et al.*, 1999; *Weissbrod and Sneh*, 2002] is actually observable on the African plate, trending NNE–SSW and E–W (reported by *Meshref* [1990]). It cannot be seen on the Arabian plate because the Precambrian arkosic sequence is buried at a depth >4 km in the Hamad basin and surrounding areas, and its relics are below the resolution of the data points. The basement in Jordan deepens gradually northward from −3 to −5 km toward the Syrian border (Figure 2). The above mentioned Hamad basin is part of a Precambrian low [*Brew et al.*, 1997], whereas the deeper Palmyrides basin, up to −10 km, is a persistent complex tectonic feature initiated in Permian times, that extends toward central Israel, [*Seber et al.*, 1993; *Laws and Wilson*, 1997; *Brew et al.*, 1999; *Segev and Eshet*, 2003]. The SW–NE Syrian arc fold belt, including the Palmyrides is the major Late Cretaceous intraplate structure that is clearly seen on the top of the basement map. The dominant Tertiary-Recent structures in the area studied are the updoming around the Red Sea spreading center, the Suez rift and the Gulf of Elat pull-apart basins, and the string of young tectonic sedimentary basins along the DST separating between the Arabian plate and the Sinai sub-plate (Figure 2). The basement step on this fault system reaches ~5 km [*Hofstetter et al.*, 2000].

Acknowledgments

[12] The authors express their thanks to L. Fleischer, Z. Ben-Avraham, Z. Garfunkel, V. Goldshmidt, Y. Rotstein, G. Shamir and U. ten Brink for fruitful discussions, and to B. Katz for editing the text. The paper was considerably improved by the comments of E. Sandvol and an anonymous reviewer.

References

Abdel Aal, A., R. J. Price, J. D. Vaitl, and J. A. Shrallow (1994), Tectonic evolution of the Nile delta, its impact on sedimentation and hydrocarbon potential, paper presented at 12th EGPC Conference, Egyptian Gen. Pet. Corp., Cairo.

Abdel Aal, A., A. El Barkooky, M. Gerrits, H. Meyer, M. Schwander, and H. Zaki (2000), Tectonic evolution of the Eastern Mediterranean basin and its significance for hydrocarbon prospectivity in the ultra deep water of the Nile Delta, *Leading Edge*, *19*(10), 1086–1102.

Abu Ollo, S., and H. El Kholy (1992), West Abu Qir discovery, its exploration, significance and case history as a part of the Nile delta exploration tasks, paper presented at 11th EGPC Conference, Egyptian Gen. Pet. Corp., Cairo.

Abu Saad, L., and I. J. Andrews (1993), A database of stratigraphic information from deep boreholes in Jordan, *Subsurface Geol. Bull.*, *6*, 182 pp., Nat. Resour. Auth., Amman, Jordan.

Alfy, M., F. Polo, and M. Shash (1992), The geology of Abu-Madi gas field, paper presented at 11th EGPC Conference, Egyptian Gen. Pet. Corp., Cairo.

Al-Zoubi, A. S., and A. T. Batauneh (1999), Two main play concepts identified in Jordan's basins, *Oil Gas J.*, *26*, 86–89.

Andrews, I. J. (1991), Palaeozoic lithostratigraphy in the subsurface of Jordan, *Subsurface Geol. Bull.*, *2*, Nat. Resour. Auth., Amman, Jordan.

Andrews, I. J. (1992a), Permian, Triassic and Jurassic lithostratigraphy in the subsurface of Jordan, *Subsurface Geol. Bull.*, *4*, 60 pp., Nat. Resour. Auth., Amman, Jordan.

Andrews, I. J. (1992b), Cretaceous and Palaeogene lithostratigraphy in the subsurface of Jordan, *Subsurface Geol. Bull.*, *5*, Nat. Resour. Auth., Amman, Jordan.

Ben-Avraham, Z. (1985), Structural framework of the Gulf of Elat (Aqaba), northern Red Sea, *J. Geophys. Res.*, *90*(B1), 703–726.

Ben-Avraham, Z., A. Ginzburg, J. Makris, and L. Eppelbaum (2002), Crustal structure of the Levant Basin, eastern Mediterranean, *Tectonophysics*, *346*(1–2), 23–43.

Bentor, Y. K. (1985), The crustal evolution of the Arabian-Nubian Massif with special reference to the Sinai Peninsula, *Precambrian Res.*, *28*, 1–74.

Beyth, M., and A. Heimann (1999), The youngest igneous event in the crystalline basement of the Arabian-Nubian shield, Timna Igneous Complex, *Isr. J. Earth Sci.*, *48*, 113–120.

Brew, G. E., R. K. Litak, D. Seber, M. Barazangi, A. Al-Imam, and T. Sawaf (1997), Basement depth and sedimentary velocity structure in the northern Arabian platform, eastern Syria, *Geophys. J. Int.*, *128*, 617–631.

Brew, G. E., R. K. Litak, M. Barazangi, T. Sawaf, and T. Zaza (1999), Tectonic evolution of northeast Syria: Regional implications and hydrocarbon prospects, *GeoArabia*, *4*, 289–318.

El Beialy, S. Y. (1988), Palynology, palaeoecology and dynocyst stratigraphy of the Oligocene trough Pliocene in the Qantara 1 well, eastern Nile delta, Egypt, *J. Afr. Earth Sci.*, *11*(3–4), 291–307.

Eyal, M., Y. Bartov, A. Shimron, and Y. Bentor (1987), The geology of Sinai—Explanatory notes on the geological photomap 1:500,000 scale (in Hebrew), in *Sinai*, vol. 1, edited by G. Gvirtzman et al., pp. 21–41, Tel-Aviv Univ., Minist. of Def., Tel-Aviv, Israel.

Folkman, Y., and R. Assael (1980), Aeromagnetic map—Sinai Peninsula, Holon, *IPRG Rep. AM/575/79*, Inst. for Pet. Res. and Geophys., Holon, Israel.

Garfunkel, Z. (1981), Internal structure of the Dead Sea leaky transform (rift) in relation to plate kinematics, *Tectonophysics*, *80*, 81–108.

Garfunkel, Z., and Y. Bartov (1977), The tectonics of the Suez rift, *Isr. Geol. Surv. Bull.*, *71*, 44 pp.

Ginzburg, A., and Y. Folkman (1979), Seismic refraction investigation of the crystalline basement under central and northern Israel, *IPRG Rep. Ref/518/79*, Inst. for Pet. Res. and Geophys., Holon, Israel.

Hofstetter, A., C. Dorbath, M. Rybakov, and V. Goldshmidt (2000), Crustal and upper mantle structure across the Dead Sea rift and Israel from teleseismic P wave tomography and gravity data, *Tectonophysics*, *327*, 37–59.

Jachens, R. C., and B. C. Moring (1990), Maps of the thickness of Cenozoic deposits and the isostatic residual gravity over basement for Nevada, *U.S. Geol. Surv. Open File Rep.*, *90–404*, 11 pp.

Laws, E. D., and M. Wilson (1997), Tectonics and magmatism associated with the Mesozoic passive continental margin development in the Middle East, *J. Geol. Soc. London*, *154*, 459–464.

Makris, J., and J. Wang (1995), Geophysical study and geodynamics of the eastern Mediterranean Sea, *Aktenzeichen Ma 719/48-1*, 135 pp., Inst. für Geophys., Univ. at Hamburg, Hamburg, Germany.

Malovitsky, Y. P., A. Esina, O. V. Kazakov, V. N. Moskalenko, and G. V. Osipov (1975), Basic features of the deep bottom structure of the Mediterranean sea-floor, *Rapp. Comm. Int. Mer Medit.*, *23*(4a), p. 125.

Meshref, W. M. (1990), Tectonic framework, in *The Geology of Egypt*, edited by R. Said, pp. 113–155, A. A. Balkema, Brookfield, Vt.

Mushkin, A., O. Navon, L. Halicz, A. Heimann, G. Woerner, and M. Stein (1999), Geology and geochronology of the Amram Massif, southern Negev Desert, Israel, *Isr. J. Earth Sci.*, *48*, 179–193.

Phillips, J. D. (1997), Potential-Field Geophysical Software for the PC, version 2.2, U.S. Dep. of the Interior, U.S. Geol. Surv., Denver, Colo.

Ryan, M. B. F. (1978), Messinian badlands on the southern margin of the Mediterranean Sea, *Mar. Geol.*, *27*, 349–363.

Rybakov, M., V. Goldshmidt, L. Fleischer, and Y. Rotstein (1999a), Crystalline basement in central Israel derived from gravity and magnetic data, *Isr. J. Earth Sci.*, *48*, 101–111.

Rybakov, M., V. Goldshmidt, Y. Rotstein, L. Fleischer, and I. Goldberg (1999b), Petrophysical constraints on gravity/magnetic interpretation in Israel, *Leading Edge*, *18*(2), 269–272.

Rybakov, M., V. Goldshmidt, L. Fleischer, and Y. Ben-Gai (2000), 3-D gravity and magnetic interpretation for the Haifa Bay area (Israel), *J. Appl. Geophys.*, *44*(4), 353–367.

Rybakov, M., L. Fleischer, and U. ten Brink (2003), The Hula Valley subsurface structure inferred from gravity data, *Isr. J. Earth Sci.*, *52*(3–4), 113–122.

Seber, D., M. Barazangi, T. A. Chaimov, D. Al-Saad, T. Sawaf, and M. Khaddour (1993), Upper crustal velocity structure and basement morphology beneath the intracontinental Palmyride fold-thrust belt and north Arabian platform in Syria, *Geophys. J. Int.*, *113*, 752–766.

Segev, A. (1987), The age of the latest Precambrian volcanism in southern Israel, northeastern Sinai and southwestern Jordan—A re-evaluation, *Precambrian Res.*, *36*, 277–285.

Segev, A. (2000), Synchronous magmatic cycles during the fragmentation of Gondwana: Radiometric ages from the Levant and other provinces, *Tectonophysics*, *325*, 257–277.

Segev, A. (2002), Flood basalts, continental breakup and the dispersal of Gondwana: Evidence for periodic migration of upwelling mantle flows (plumes), *Stephan Mueller Spec. Publ. Ser.*, vol. 2, pp. 171–191, Eur. Geosci. Union, Strasbourg, France.

Segev, A., and Y. Eshet (2003), Significance of Rb/Sr age of Early Permian volcanics, Helez Deep 1A borehole, central Israel, *Afr. Geosci. Rev.*, *10*(4), 333–345.

Segev, A., V. Goldshmidt, and M. Rybakov (1999), Late Precambrian-Cambrian tectonic setting of the crystalline basement in the northern Arabian-Nubian Shield as derived from

gravity and magnetic data: Basin-and-range characteristics, *Isr. J. Earth Sci.*, *48*, 159–178.

Segev, A., M. Rybakov, V. Lyakhovsky, A. Hofstetter, G. Tibor, and Z. Ben Avraham (2003), The Levant and southeastern Mediterranean lithospheric structure and isostatic compensation since the Pliocene times, paper presented at EGS-AGU-EUG Joint Assembly, Eur. Geosci. Union, Nice, France.

Sengör, A. M., Y. Yilmaz, and O. Süngürlu (1984), Tectonics of the Mediterranean Cimmerides: Nature and evolution of the western termination of Palaeo-Tethys, in *The Geological Evolution of the Eastern Mediterranean*, edited by J. E. Dixon and A. H. F. Robertson, *Geol. Soc. Spec. Publ.*, *17*, 77–112.

Stampfli, G. M. (2000), Tethyan oceans, in *Tectonic and Magmatism in Turkey and the Surrounding Area*, edited by E. Bozkurt, J. A. Winchester, and J. D. A. Piper, *Geol. Soc. Spec. Publ.*, *173*, 1–23.

Stein, M., and S. L. Goldstein (1996), From plume head to continental lithosphere in the Arabian-Nubian shield, *Nature*, *382*, 773–778.

Stern, R. J. (1994), Arc assembly and continental collision in the Neoproterozoic East African Orogen: Implication for the consolidation of Gondwanaland, *Annu. Rev. Earth Planet. Sci.*, *22*, 319–351.

ten Brink, U., M. Rybakov, A. Al-Zoubi, M. Hassouneh, U. Frieslander, A. Batayneh, V. Goldshmidt, M. Daoud, Y. Rotstein, and J. K. Hall (1999), The anatomy of the Dead Sea plate boundary: Does it reflect continuous changes in plate motion?, *Geology*, *27*(10), 887–890.

Trachtman, P., Y. Rotstein, and U. Frieslander (1990), Deep crustal reflections in the coastal plain of Israel, *IPRG Rep. 894/415/90*, 4 pp., Inst. for Pet. Res. and Geophys., Holon, Israel.

Weber, M., and DESERT Group (2004), The crustal structure of the Dead Sea Transform, *Geophys. J. Int.*, *156*, 655–681.

Weissbrod, T., and A. Sneh (2002), Sedimentology and paleogeography of the Late Precambrian-Early Cambrian arkosic and conglomeratic facies in the northern margins of the Arabo-Nubian Shield, *Isr. Geol. Surv. Bull.*, *87*, 44 pp.